

# TRANSVERSE SCHOTTKY AND BTF MEASUREMENTS AND SIMULATIONS IN SPACE-CHARGE AFFECTED COASTING ION BEAMS

S. Paret, V. Kornilov, O. Boine-Frankenheim, GSI, Darmstadt, Germany  
T. Weiland, Technische Universität Darmstadt, Darmstadt, Germany

## Abstract

A study of the transverse dynamics of coasting ion beams with moderate space charge is presented. An analytic model based on the dispersion relation with a linear space-charge force is used to describe the impact of space charge on transverse beam transfer functions (BTFs) and the stability limits of a beam. The dielectric function obtained in this way is employed to describe the transverse Schottky spectrum with linear space charge as well. The difference between space charge and impedance effects is highlighted. An experiment performed in the heavy ion synchrotron SIS-18 at GSI to detect space-charge effects at different beam intensities is explicated. The measured transverse Schottky spectra, BTFs and stability diagrams are compared with the analytic model. The space-charge parameters evaluated from the Schottky and BTF measurements are compared with estimations based on measured beam parameters. Furthermore, particle tracking simulations demonstrating the impact of collective effects on the Schottky and BTF diagnostics are presented. The simulation results are used to verify the space-charge model.

## INTRODUCTION

GSI's heavy ion synchrotron SIS-18 will serve as a booster for the projected FAIR accelerators [1]. For this purpose, the linear accelerator UNILAC and SIS-18 have to accelerate beams of unprecedented intensity. The accompanying collective effects may degrade the beam quality and cause particle losses due to instabilities. Therefore collective effects in ion beams are investigated at GSI.

In SIS-18, where the particle energy is low, space charge is a major concern as it is known to inhibit Landau damping of coherent beam instabilities [2, 3]. Furthermore the output of standard diagnostic tools for the accelerator operation, like Schottky diagnostics and beam transfer functions (BTFs), has to be interpreted taking into account space-charge effects. As shown in this report, an analytic model, related to the well known model for impedances, can be used to describe the impact of space charge on transverse Schottky or BTF signals as long as the nonlinear components of the self-field can be neglected. It allows also to retrieve the fractional part of the working point which cannot be read directly from the signals due to an intensity dependent distortion. In the next section this model introduced. The following sections an experiment and computer

simulations are described and their output is compared to the space-charge model. A more detailed discussion of the topics of this article can be found in Refs. [4, 5, 6].

## LINEAR SPACE CHARGE AND BEAM DIAGNOSTICS

The current fluctuation in a coasting ion beam produces a longitudinal Spectrum, consisting of a series of bands at integer multiples,  $m$ , of the revolution frequency  $f_0$ . Due to the incoherent betatron motion of the particles a fluctuation of the beam's dipole moment arises and leads to the transverse Schottky spectrum. At low intensity the side bands forming this spectrum are located at frequencies [7]

$$f_m^\pm = f_0(m \pm Q_f), \quad (1)$$

where the  $+$  refers to the upper side band of the  $m^{\text{th}}$  longitudinal band and the  $-$  to the corresponding lower side band.  $Q_f$  is the fractional part of the working point.

The Schottky bands of a beam devoid of collective effects reflect the momentum distribution of the beam. The rms width of the longitudinal Schottky spectrum reads

$$\sigma_m = m|\eta|f_0\sigma_p, \quad (2)$$

where we introduced the slip factor  $\eta$  and the relative momentum spread  $\sigma_p$ . The rms width of the side bands depends in addition on the full tune  $Q$  and the chromaticity  $\xi$  by virtue of

$$\sigma_{m,0}^\pm = |m \pm (Q_f\eta - \xi Q)|f_0\sigma_p. \quad (3)$$

Exciting a Schottky side band with noise or a time harmonic signal and division of the response by the excitation yields the transverse BTF [8]

$$r_0(z) = \mp \int_{-\infty}^{\infty} \frac{P_0(\tilde{z})}{z - \tilde{z}} d\tilde{z} \quad (4)$$

where  $z = (f_{m,0}^\pm - f)/\sigma_m^\pm$  is the normalized frequency,  $P_0$  the Schottky side band under consideration and  $z$  the particle momentum divided by  $\sigma_p$ . The BTF of a beam with a Gaussian momentum distribution is the complex error function [9],

$$r_0(z) = \mp i \sqrt{\frac{\pi}{2}} \left[ 1 - \operatorname{erf} \left( \frac{iz}{\sqrt{2}} \right) \right] e^{-z^2/2}. \quad (5)$$

A dipolar transverse impedance  $Z_{\perp}$  deforms the BTF according to [8]

$$r(z) = \frac{r_0(z)}{1 - (\Delta U + i\Delta V)r_0(z)}. \quad (6)$$

Here we introduced the real parameters  $\Delta U$  and  $\Delta V$  which express the action of the real and imaginary part of the impedance. They are defined by

$$\Delta U + i\Delta V = \frac{r_p Z^2 N f_0}{2\pi Z_0 A Q \gamma \sigma_m^{\pm}} (\text{Im}(Z_{\perp}) + i\text{Re}(Z_{\perp})), \quad (7)$$

where  $N$  is the particle number,  $Z$  the charge number,  $A$  the mass number,  $Z_0$  the vacuum impedance and  $\gamma$  the Lorentz factor.  $\Delta U$  is linked to the coherent tune shift due to  $\text{Im}(Z_{\perp})$  and  $\Delta V$  to the growth rate of instability due to  $\text{Re}(Z_{\perp})$ . The same parameters can be used to describe the Schottky side bands of a beam affected by an impedance. Their shape then follows [7]

$$P(z) = \frac{P_0(z)}{|1 - (\Delta U + i\Delta V)r_0(z)|^2}. \quad (8)$$

The action of a dipolar impedance is coherent, i.e. representable by a force acting on the barycenter of the beam. On the contrary the space charge as it is incoherent. Comparing the equation of motion of a particle in a constant focusing channel that is perturbed either by an impedance or space charge gives insight into the relation between the two effects [9]. The dispersion relation Eq. 6 is found by averaging of the equations of motion

$$\ddot{x}_i + \omega_{\beta,i}^2 x_i = K_{imp} \langle x \rangle \quad (9)$$

of all particles forming a beam.  $K_{imp}$  is the force acting on the particle  $i$  due to the impedance. The angular brackets stand for the average over all particles.

Under the influence of a linear space-charge force, the equation of motion assumes the form

$$\ddot{x}_i + \omega_{\beta,i}^2 x_i = K_{sc}(x - \langle x \rangle) \quad (10)$$

from which follows

$$\ddot{x}_i + (\omega_{\beta,i} - \Delta\omega_{sc})^2 x_i = K_{sc} \langle x \rangle \quad (11)$$

in first order. The frequency shift due to space charge is given by  $K_{sc}/(2\omega_{\beta})$ . The resulting space-charge tune-shift in the vertical plane in a coasting beam reads [10]

$$\Delta Q_{sc,y} = \frac{r_p Z^2 N g}{\pi \beta^2 \gamma^3 A (\epsilon_y + \sqrt{\epsilon_y \epsilon_x \beta_x / \beta_y})}, \quad (12)$$

where  $\beta_y$  is the mean vertical beta function,  $\epsilon_y$  the full vertical emittance.  $\beta_x$  and  $\epsilon_x$  are the corresponding parameters in the horizontal plane.  $g$  is the form factor which depends on the transverse particle distribution, being 1 for a KV beam. Gaussian beams are approximated with  $g = 2$

and using the  $2\sigma$  emittances. We define the *space-charge parameter* for a given lower or upper side band as

$$\Delta U_{sc} = \frac{\Delta Q_{sc} f_0}{\sigma_m^{\pm}}. \quad (13)$$

Formally Eq. 11 differs from Eq. 9 only by the shift of  $\omega_{\beta,i}$ . It can be shown that this frequency shift translates into a shift of the argument  $z$  towards [3, 4, 5]

$$z_{sc} = z \mp \Delta U_{sc} \quad (14)$$

on the right hand side of Eq. 6 and Eq. 8. Combining the impact of an impedance and space charge results in

$$r(z) = \frac{r_0(z_{sc})}{1 - (\Delta U + i\Delta V - \Delta U_{sc})r_0(z_{sc})} \quad (15)$$

and

$$P(z) = \frac{P_0(z_{sc})}{|1 - (\Delta U + i\Delta V - \Delta U_{sc})r_0(z_{sc})|^2}. \quad (16)$$

These two equations indicate that  $\Delta U_{sc}$  causes a mirror inverted distortion compared to  $\Delta U$  given the same sign. Only space charge shifts  $P_0$  and  $r_0$  — this is a qualitative difference to impedance effects. Treating space charge like an impedance (with opposite sign), which is often done, attributes the signal an incorrect position in frequency space.

Taking the inverse of Eq. 15,

$$\frac{1}{r(z)} = U(z_{sc}) + iV(z_{sc}) \quad (17)$$

$$= \frac{1}{r_0(z_{sc})} + \Delta U_{sc} - \Delta U - i\Delta V, \quad (18)$$

we obtain the stability diagram. As the stability diagram is a parametric plot of  $U(z_{sc})$  and  $V(z_{sc})$  the distinct frequency shift due to space charge is not visible in this representation. What remains is a shift of the stability diagram like the one caused by an imaginary impedance.

## MEASUREMENT OF SPACE CHARGE

A dedicated experiment for the observation of space-charge effects was accomplished in SIS-18. For this purpose a  $^{40}\text{Ar}^{18+}$  beam was stored for several seconds at the injection energy before acceleration. This time was needed to improve the statistics of the Schottky measurements and to provide enough time for the frequency sweep when BTFs were measured. The injection energy of SIS-18 is 11.4 MeV/u, corresponding to  $\gamma = 1.012$  or  $\beta = 0.15$ . The associated revolution frequency is  $f_0 = 214$  kHz. The number of stored particles was varied from  $2.5 \times 10^8$  to  $1.1 \times 10^{10}$  ions by adjusting the beam current in UNILAC.

A system for Schottky and BTF diagnostics, developed for the experimental storage ring (ESR) at GSI, was replicated for SIS-18 [11]. For the BTF detection a strip-line kicker transmits the exciting signal from a network analyzer to the beam. The signal of the beam is picked up

by a plate capacitor and acquired by the network analyzer. Schottky spectra are obtained connecting a spectrum analyzer to the pick-up. The sensitivity of the diagnostic hardware goes down at low frequencies. On the other hand, at high frequencies the interaction parameters become small as  $\sigma_m^\pm$  increases. A frequency of about 10 MHz, corresponding to  $m = 50$ , was used as a compromise. The measurements were done in the vertical plane where the smaller gap between the detector plates promised a better signal to noise ratio.

Longitudinal Schottky spectra were recorded to provide a reference for  $\sigma_p$  and  $f_0$ . Though they are contained in the transverse spectra and BTFs, in practice it is easier to extract  $Q_f$  and  $\Delta Q_{sc}$  with the other parameters known. It turned out that  $f_0$  and  $\sigma_p$  depend on the intensity. Collective effects in UNILAC and the transfer channel leading to SIS-18 are held responsible for this behavior, but the investigation of this issue is ongoing.

In order to estimate the expected collective effects, the beam current, providing  $N$ , was detected, as well, with a transformer. Beam profiles were measured to determine the emittance. For this purpose an ionization profile monitor [12] (IPM) was employed. From the measured profiles the transverse emittances were calculated using  $\epsilon_y = 4a_y^2/\beta_y$  with  $\beta_y$  computed with a beam optics code. In the IPM an electrostatic field transversally accelerates rest gas molecules that were ionized in collisions with beam particles. These molecules hit the so called micro channel plated which in turn emit a large number of electrons which are collected on a wire array.

The measured profiles are approximately Gaussian shaped. The resulting emittance did not change significantly during the experiment and amounted to  $\epsilon_y \approx 4.4$  mm mrad and  $\epsilon_x \approx 6.0$  mm mrad. Due to the different mean beta functions in the two planes, Eq. 12 could be approximated by

$$\Delta Q_{sc,y} = \frac{r_p Z^2 N g}{2\pi \beta^2 \gamma^3 A \epsilon_y} \quad (19)$$

with an error of a few percent.

With  $N$ ,  $\epsilon_y$  and  $\sigma_p$  one can estimate  $\Delta Q_{sc}$  and  $\Delta U_{sc}$ . Table 1 lists these estimations with the measured beam parameters. Also  $\Delta U$  and  $\Delta V$  were estimated for a perfectly conducting beam pipe and with the calculated impedances of the extraction kickers and the resistive wall. Both parameters are negligible compared to  $\Delta U_{sc}$  and therefore are not considered in the following discussion.

The lower Schottky side bands of  $m = 50$  measured at three intensities are displayed in Fig. 1. At low intensity the band is symmetric and well described by a Gaussian function. With increasing particle number the symmetry is lost and the band becomes narrower, despite the increasing momentum spread. Equation 16 was fitted to the data with three parameters of freedom: Amplitude,  $f_m^\pm$  and  $\Delta U_{sc}$ .  $\sigma_p$  was set to the value found in the longitudinal measurement. A very good agreement with the data is observed up to the maximal beam intensity.

Table 1: Measured particle numbers and momentum spreads together with the corresponding tune shift and space-charge parameter.

$N / 10^9$	$\delta p/p / 10^{-4}$	$\Delta Q_{sc,est}$	$\Delta U_{sc,est}$
0.25	2.5	0.001	0.09
0.45	2.8	0.002	0.15
0.90	4.2	0.004	0.19
2.0	5.6	0.010	0.32
3.9	6.7	0.019	0.53
7.	7.6	0.034	0.84
10.	7.8	0.048	1.2
11.	7.8	0.053	1.3

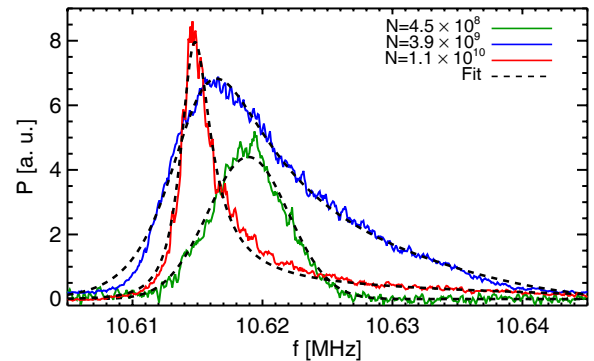


Figure 1: Measured lower Schottky bands at different beam intensities with fitted model. The shift of  $f_0$  is compensated in this figure.

The BTF data were analyzed fitting Eq. 15 by the amplitude and the phase. Both the data and the fit are shown in Fig. 2. The corresponding stability diagrams are visualized in Fig. 3. At low and moderate intensity the fitted curves agree well with the data. At high intensity, however, only a partial agreement can be stated. In particular the sharp peak in the maximum is not well reproduced. The stability diagrams are evidently shifted and keep their shape, as expected. With increasing beam intensity the noise on the stability diagram grows.

The space-charge parameters from the estimation,  $\Delta U_{sc,est}$ , and from the fit,  $\Delta U_{sc,shape}$ , are plotted in Fig. 4. Taking advantage of the known low intensity tune,  $Q_{f,0}$ , there is another way to determine the space-charge parameter—as long as impedances are negligible. Using Eq. 13 we find

$$\Delta U_{sc,shift} = \frac{Q_{f,0} - Q_f}{\sigma_m^\pm}. \quad (20)$$

$\Delta U_{sc,shift}$  and  $\Delta U_{sc,shape}$  coincide if the measurement is consistent, which is confirmed by the experimental data. The BTF data indicate slightly larger values, but due to the better agreement between the Schottky data and the model, the latter seem to be more reliable. A precise explanation for this difference was not found. It is reasonable, though, to assume that high intensity beams were close to a coher-

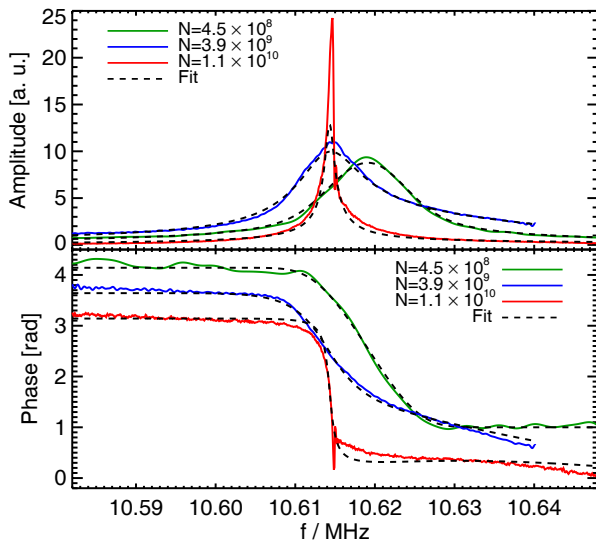


Figure 2: BTFs measured with the same settings as the Schottky bands in Fig. 1.

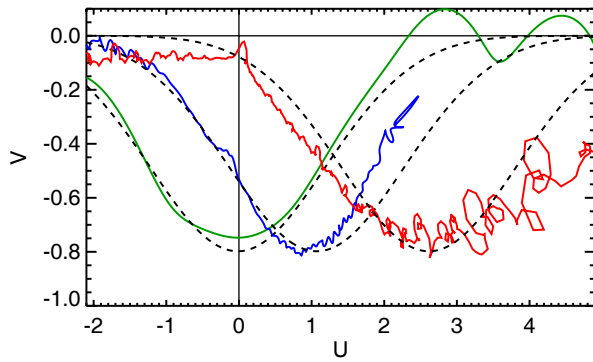


Figure 3: Measured stability diagrams. The color code is the same as in the previous figures.

ent instability. In this case the response to the excitation may become nonlinear so that a base assumption of the BTF theory is violated.

$\Delta U_{sc,est}$ , however, is significantly smaller. The discrepancy exceeds the estimated measuring uncertainty, which is discussed in Ref. [6]. A possible error of the calculated beta function at the location of the IPM is not included in the error estimation, though. As the beta function was not measured, a systematic deviation of the assumed emittances could occur and explain the observed deviation. It was tried to model the impact of a nonlinear amplification of the micro channel plates in the IPM, since their performance degrades with time. However, this approach did not explain the observations, and was itself affected with large uncertainties.

Employing Eq. ??,  $\Delta U_{sc}$  one can calculate  $\Delta Q_{sc}$ . Even the low intensity tune can be extracted from a high intensity measurement using  $Q_{f,0} = Q_f + \Delta U_{sc} \sigma_m^\pm$ . The expected

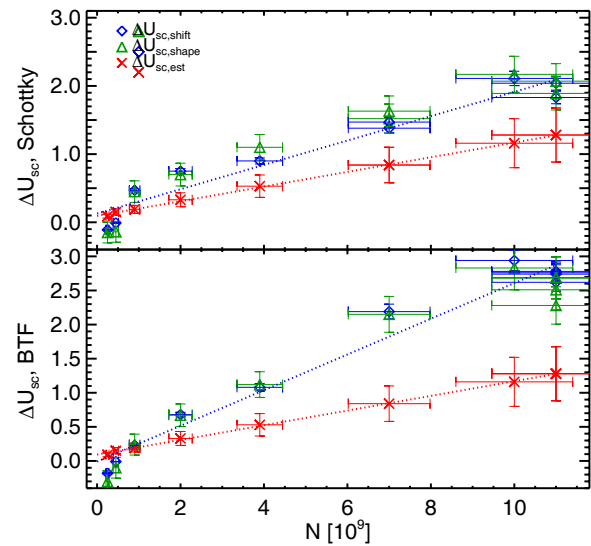


Figure 4: Measured and estimated space-charge parameters.

linear decrease of  $Q_f$  with increasing intensity and the consistency with the constant  $Q_{f,0}$  are well confirmed by the experimental data.

## SIMULATION RESULTS

Particle tracking simulations were performed in a constant focusing channel with a code developed for this purpose. The fluctuation of the macro-particle density in a random distribution yields a fluctuating current dipole moment whose Fourier transform is the transverse Schottky spectrum. In order to simulate a BTF, the side band is excited with white noise.

KV and Gaussian particle distributions were simulated up to  $\Delta U_{sc} = 2$ . Equation 16 and Eq. 15, respectively, were fitted to the simulation output. An excellent agreement of the fit parameters with the simulation settings, as well as between the data and the fitted curve, was found for all settings.  $\Delta U_{sc}$  from the fit differed by maximal 4% from the expected values only. No significant deviations between KV and Gaussian beams were found. In Fig. 5 the simulation results with  $\Delta U_{sc} = 2$  are shown.

The impact of an imaginary impedance was studied as well by means of numerical simulations. Going beyond the scope of the feasible in our experiments, the impact of an imaginary impedance was compared to the one of space charge by virtue of numerical simulations. One showcase example can be seen in Fig. 6. These simulations were done with  $\Delta U = 2$  and either  $\Delta U_{sc} = 0$  or  $\Delta U_{sc} = 2$ , as well. In the first case, the deformation is mirror inverted with respect to the space-charge effect and the signal is shifted considerably farther. In the second case, the deformations cancel each other and the signal is shifted only. All predictions of the linear space-charge model are well confirmed by the simulations.

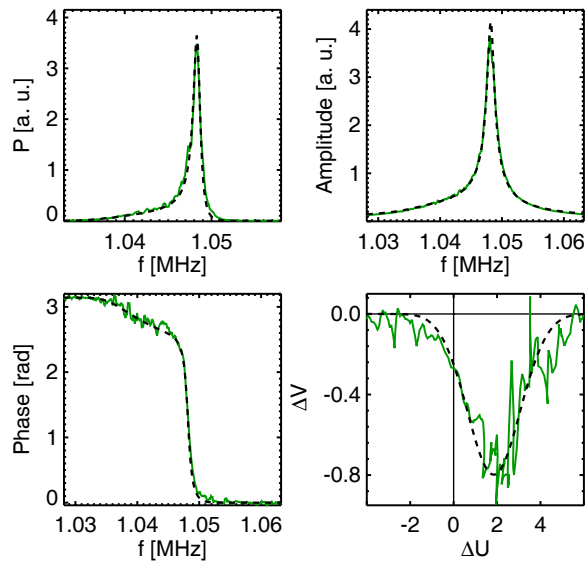


Figure 5: Simulation results of a beam with Gaussian transverse profile and  $\Delta U_{sc} = 2$ . On top a Schottky band (left) and the BTF amplitude are shown. On bottom follow the BTF phase and the stability diagram (right).

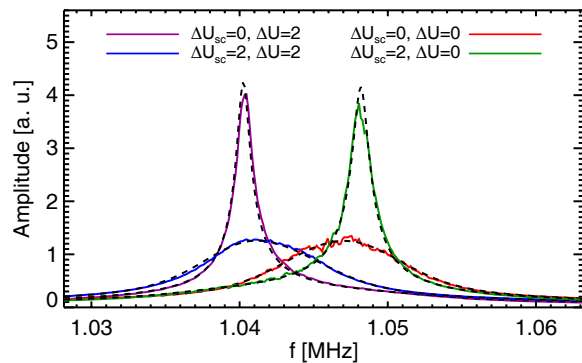


Figure 6: Simulated BTF amplitude with different  $\Delta U_{sc}$  and  $\Delta U$  settings. The dashed lines represent the fitted model.

## CONCLUSIONS

A linear space-charge model was discussed and employed to describe the transverse Schottky spectra and BTFs of intense coasting beams. The data from experiments in SIS18 partially agree well with this model, but some discrepancies were noticed. Using the model,  $Q_f$ ,  $\Delta Q_{sc}$  and the  $\Delta U_{sc}$  were determined from the measured data. Computer simulations were accomplished to study the space charge and impedance effects. The simulation results are very well described by the model. Within the limits of the linear approximation the model proved to be useful. For daily use the reliability of measurements needs improvements. For tune measurements a higher frequency with smaller  $\Delta U_{sc}$  is preferred.

## REFERENCES

- [1] FAIR Baseline Technical Report, GSI, 2006, <http://www.gsi.de/fair/reports/btr.html>
- [2] A. Hofmann, Tune shifts from self-fields and images, CAS: 5th General Accelerator Physics Course, 94-01\_v1, 1994
- [3] D. V. Pestrikov, Self-consistent dipole coherent oscillations of a coasting ion beam with strong space charge, Nucl. Instr. and Methods, 578, 1, 2007
- [4] O. Boine-Frankenheim, V. Kornilov and S. Paret, Measurement and simulation of transverse Schottky noise with space charge, Phys. Rev. ST Accel. Beams, 11, 7, 2008
- [5] S. Paret, V. Kornilov, O. Boine-Frankenheim and T. Weiland, Transverse Schottky and beam transfer function measurements in space charge affected coasting ion beams, Phys. Rev. ST Accel. Beams, 13, 2, 2010
- [6] S. Paret, Transverse Schottky spectra and beam transfer functions of coasting ion beams with space charge, Ph.D. thesis, Technische Universität Darmstadt, 2010, <http://tuprints.ulb.tu-darmstadt.de/2134/>
- [7] S. Chattopadhyay, Some Fundamental Aspects of Fluctuations and Coherence in Charged-Particle Beams in Storage Rings, Technical report no. CERN 84-11, CERN, 1984
- [8] A. W. Chao, Physics of Collective Beam Instabilities in High Energy Accelerators, Wiley, 1993
- [9] K. Y. Ng, Transverse Instability at the Recycler Ring, Technical report, FERMILAB-FN-0760-AD, FNAL, 2004
- [10] K. Schindl, Space charge, CERN Accelerator School: Basic Course on General Accelerator Physics, CERN-PS-99-012-DI, 1999
- [11] U. Schaaf, Schottky-Diagnose und BTF-Messungen an gekühlten Strahlen im Schwerionenspeicherring ESR, Universität Frankfurt, GSI-91-22, 1991
- [12] M. Schwickert, P. Forck, P. Kowina, T. Giacomini, H. Reeg and A. Schlörit, Beam diagnostic developments for FAIR, DIPAC09, 2009